An in silico study to inspect the induction of ferroptosis by Gossypol on the human ovarian teratocarcinoma cell line PA-1

A Dissertation Report by
Akhil V Hothi
Enrollment No. - 210621018
MSc Biotechnology, Semester IV

Under the supervision of
Dr Anmol Kumar
Assistant Professor
Department of Biotechnology
Atmiya University
'Yogi Dham Gurukul' Kalawad Road
Rajkot (Gujarat) – 360005

2022-2023

C E R T I F I C A T E

This is to certify that this dissertation work entitled **"An in silico study to inspect the induction of ferroptosis by Gossypol on the human ovarian teratocarcinoma cell line PA-1"** was successfully carried out by **Akhil Hothi** towards the partial fulfillment of requirements for the degree of Bachelor of Science in Biotechnology of Atmiya University Rajkot. It is an authentic record of his own work, carried out by him under the guidance of **Dr Anmol Kumar** during the academic year of **2022-2023**. The content of this report, in full or in parts, has not been submitted for the award of any other degree or certificate in this or any other University.

Dr Nutan Prakash Vishvakarma
Head of the Department

Dr Anmol Kumar
Guide

D E C L A R A T I O N

I, Akhil Vijaybhai Hothi, hereby declare that the work incorporated in the present dissertation report entitled **"An in silico study to inspect the induction of ferroptosis by Gossypol on the human ovarian teratocarcinoma cell line PA-1"** is my own work and is original. This work (in part or in full) has not been submitted to any University for the award of any Degree or a Diploma.

Date: 07/04/2023 **Student Name:** Akhil V Hothi

An in silico study to inspect the induction of ferroptosis by Gossypol on the human ovarian teratocarcinoma cell line PA-1

Abstract

Cancer remains the second leading cause of death worldwide, with ovarian cancer accounting for approximately 300,000 new cases and 200,000 deaths in 2020. Ovarian Teratocarcinoma is a rare, malignant form of this disease, characterized by the presence of various tissue types within a tumor. Gossypol, a natural polyphenolic compound found in cotton seeds, has been shown to exhibit anti-proliferative and anti-metastatic properties against different types of human cancers. In this study, in silico analysis is performed using molecular docking tools, PyRx® and AutoDock Vina®, to identify target proteins involved in ferroptosis regulation that were abnormally expressed. Visualization of the obtained results is performed using PyMOL. The results indicate that Gossypol demonstrated high binding efficacy with these proteins, as evidenced by the strong negative binding affinity. In conclusion, Gossypol has the potential to alter the function of these target proteins and inhibit their proliferative activity. Further validation through in vitro studies on cell lines is necessary. This research contributes to the understanding of ovarian cancer and may lead to the development of novel treatments for this devastating disease.

Keywords: Human ovarian teratocarcinoma, PA1 cell line, Gossypol, Anti-proliferative, Molecular Docking.

Introduction

In 2020 over 19 million people were diagnosed with different types of cancer and approximately 9.9 million people died due to the cancer. In 2020, approximately 300,000 new cases and 200,000 died due to ovarian cancer[1]. Ovarian Teratocarcinoma is a rare, malignant form of this disease, characterized by the presence of various tissue types within a tumor. Ferroptosis is non-apoptotic form of programmed cell death. Ferroptosis is characterized by the accumulation of intracellular redox active iron and ROS. Hallmarks of ferroptosis includes increase in intracellular iron concentration, defective ROS repair mechanism and presence of poly unsaturated phospholipids[2,3].

Mutation in genes such as BRCA1, BRCA2, CDKN2A, RB1 and PIK3CA are detected in PA1 cell line. Other genes like KRAS, TP53 and PTEN are also mutated in PA1 cell line. In these genes, TP53 codes for p53 protein which is indirectly involved in regulation of the ferroptosis by regulation of enzymes involved in lipid metabolism such as ACSL4[4]. Molecular docking analysis of molecules such as p53 (product of TP53), mTORC1, mTORC2, HRas, β-

Catenin, γ-secretase, STAT3 etc have been already done previously. Focus of this study is on the molecules that are over expressed in PA1 cell line and involved in ferroptosis– MEX3A, Ezrin, TfR1, Cofilin1, ANX2, HSP70 and COX2. Following is the detailed discussion of these molecules[5–13].

1. MEX3A

MEX3A protein is recently found to be suppressing ferroptosis via p53 degradation and promoting tumorigenesis in ovarian cancer. MEX3A protein's E3 ligase function is responsible for regulation of p53. Protein p53 is involved in regulation of ferroptosis in both pro-death and pro-survival functions. The p53 inhibits DPP4 (Dipeptidyl-peptidase 4) that is involved in induction of the ferroptosis. Another way by which p53 suppresses ferroptosis is by activation of CDKN1A gene that inhibits ferroptosis. Degradation of p53 leads to suppression of ferroptosis in different ways. SLC7A11 is the gene responsible for the synthesis of System X_c^- (A cystine/glutamate antiporter) that is crucial for activity of GPX4 (Glutathione Peroxidase 4) which plays essential role for peroxidation of ROS (Reactive Oxygen Species). ROS is important for the induction of ferroptosis and it mainly involved in disruption of plasma membrane. The p53 protein downregulates the expression of SLC7A11 resulting in low presence of System X_c^- on plasma membrane and lower levels of active GPX4 and thus induction of ferroptosis. Thus when p53 is degraded then GPX4 levels increases and it results in suppression of ferroptosis. The p53 also increases the expression of SAT1 and GLS2, both of them are pro-ferroptotic and thus degradation of p53 results in suppression of ferroptosis.[5]

2. Ezrin

miR-211-5p mediated Ezrin is found to be involved in regulation of the tumor proliferation and cisplatin resistance in tongue cancer. It is also found that Ezrin is involved in regulation of ferroptosis in acute compartment syndrome. Nfe2l2/Hmox1 signalling pathway is involved in regulation of ferroptosis mediated by Ezrin/Fak/Src signalling.[6,7,14]

3. TfR1

TfR1 facilitates the uptake of iron into cells by binding to transferrin, which transports iron in the blood. Research indicates that TfR1 expression increases in cells undergoing ferroptosis, indicating that iron uptake may contribute to this process. Additionally, TfR1 is believed to play a role in regulating lipid peroxidation, a critical aspect of ferroptosis. It is thought that TfR1 may transport iron to specific regions of the cell where lipid peroxidation occurs, ultimately promoting ferroptosis.[8]

4. Cofilin1

Cofilin1 is an actin binding protein that plays a role in cytoskeletal dynamics, cell migration, and cell signalling. Recently, studies have suggested that cofilin1 may also play a role in ferroptosis. A study showed that cofilin1 interacts with the lipid peroxidation regulator ACSL4, which is essential for the accumulation of polyunsaturated fatty acids (PUFAs) in the phospholipid membrane, and enhances lipid peroxidation by increasing ACSL4 activity. Another study showed that cofilin1 promotes the translocation of the lysosomal iron transporter ZIP14 to the plasma membrane, which leads to increased iron uptake and lipid peroxidation.[10,15]

5. ANX2

ANXA2 has been found to interact with the transferrin receptor (TfR1), which is responsible for the uptake of iron-bound transferrin into cells. By promoting the internalization of transferrin-bound iron, ANXA2 can increase the intracellular concentration of iron and promote ferroptosis. ANXA2 has also been shown to regulate the activity of GPX4. ANXA2 has been found to also interact with the lipoxygenase (LOX) enzyme, which catalyzes the formation of lipid peroxides.[11]

6. HSP70

In addition to its chaperone activity, HSP70 has been implicated in the regulation of cell death pathways, including ferroptosis. One of the mechanisms by which HSP70 protects cells from ferroptosis is through its interaction with and regulation of the cystine/glutamate antiporter System X_c^-. The activity of System X_c^- is required for the production of the antioxidant glutathione, which helps to prevent the accumulation of lipid peroxides. HSP70 has been shown to regulate the expression and activity of System X_c^- in response to oxidative stress, thereby preventing ferroptotic cell death.[12]

7. COX2

Recent studies have shown that COX-2/PGE2 pathway is involved in regulation of the ferroptosis. These studies concluded that COX-2 suppresses the ferroptosis by inducing the production of PGE2. The PGE2 protein is secreted by the cells and detected by EP3 and EP4 receptors. EP3 is involved in reduction of intracellular redox active iron. EP4 is involved in activation of GPX4-GSH complex that is involved in ROS repair. Thus COX2 suppresses ferroptosis by reducing intracellular iron and inducing ROS repair mechanism.[16]

In this study a single ligand molecule – Gossypol – is used to determine its ability to induce ferroptosis in PA1 cell line. All above mentioned proteins were used one by one as macromolecules to perform the docking with Gossypol.

Gossypol

Gossypol is plant polyphenolic secondary metabolite and present in *Gossypium hirtusum* L(cotton) seeds in very little amount[17]. Studies shows that Gossypol has anti-proliferative and anti-metastatic effects against many cancer types[18]. In vitro study shows that it is an effective anti-cancer agent against TNBC as it is induce the apoptosis[19].

This study focuses on *In silico* analysis of small molecule Gossypol with different target proteins or macromolecules those are involved in the regulation of ferroptosis in PA1 cell line. Molecular docking is useful to estimate the binding affinity of ligand and its target protein in different conformation. Based on these binding affinity data, hypothesis can be made that our ligand (Gossypol) can or can't bind to particular target *In vitro* or *In vivo* and it can be inhibited or induce some cascade that can be used in treatment of PA1 like ovarian teratocarcinoma. Further validation is required on these dry lab data by *In vitro* studies. This research contributes towards the developments in the fields of drug discovery and precision medicine.

Tools & Resources

1. PubChem

PubChem is a database managed by the National Centre for Biotechnology Information that stores information about the biological activities of chemical molecules. The Gossypol ligand structure was obtained from PubChem for use in molecular docking.[20]
(URL: https://pubchem.ncbi.nlm.nih.gov) [Figure:1]

2. RCSB PDB

RCSB PDB is a repository of three-dimensional structural data for macromolecules, including nucleic acids and proteins. Protein structures were acquired from RCSB PDB for use in docking analysis.[21] (URL: https://www.rcsb.org) [Figure:2]

3. AutoDock Vina

AutoDock Vina is a free and open-source software tool created by Dr Oleg Trott at The Scripps Research Institute that is used for molecular docking.[22] (URL: http://vina.scripps.edu) [Figure:3]

4. PyRx

PyRx is essentially a Graphical User Interface that uses a large body of established open-source software like AutoDock 4 and AutoDock Vina. It is a virtual Screening tool for Computational Drug Discovery that can be used to screen libraries of compounds against potential drug targets. For this study PyRx 0.8 version is used.[23]
(URL: https://pyrx.sourceforge.io) [Figure:4]

5. PyMOL

PyMOL is an open source molecular visualization system created by Warren Lyford DeLano. It is maintained and distributed by Schrödinger, Inc. PyMOL can produce 3D images of small molecules and biological macromolecules, such as proteins. For this study PyMOL 2.4.2 version is used.[24] (URL: https://pymol.org) [Figure:5]

6. AlphaFold Protein Structure Database

The AlphaFold Protein Structure Database (APSD) contains protein structures that have not been experimentally determined, but have instead been predicted using Deepmind's AlphaFold and AlphaFold2 algorithms. This database is particularly useful for research purposes when proteins are not available in the RCSB PDB. For this study, several proteins are selected from APSD that are relevant to our research goals.[25–27]
(URL: https://alphafold.ebi.ac.uk/) [Figure:6]

7. COSMIC

COSMIC (Catalogue Of Somatic Mutations In Cancer) is the world's largest and most comprehensive resource for exploring the impact of somatic mutations in human cancer. COSMIC is database is used to find different mutation in proteins of PA1 cell line.[4]
(URL: https://cancer.sanger.ac.uk/cosmic) [Figure:7]

Methods

1. Screening, Selection and Retrival of 3D Structures of Target Molecules :

For this study various databases are used such as PubMed and other services like Google Scholar to find the protein molecules that are involved in the regulation of the ferroptosis and found mutated or its expression is altered in PA1 cell line.

For the detection of mutated protein in PA1 cell line COSMIC database has been used. For screening of the various molecules having altered expression in PA1 cell line, PubMed and Google Scholar are used. Seven different protein molecules were selected that are involved in the regulation of the ferroptosis and are also having altered expression in PA1 cell line.

Retrieval of the 3D structures of the proteins is from two major databases, PDB and APSD. The PDB database is the database for experimentally derived 3D structure of proteins and associated molecules. These methods are mainly NMR, X-ray crystallography and electron microscopy. APSD on the other hand contains computationally predicted 3D structures of the proteins. In this study APSD is used to retrieve the protein structures that are currently not determined experimentally.

2. Molecular Docking :

The docking program used for this study was AutoDock Vina[7], which was integrated into PyRx. The following steps were taken for the docking process:

- → The Gossypol molecule was first energy-minimized in PyRx using Open Babel.
- → Each molecule was then loaded into the AutoDock macromolecules tab.
- → A specific macromolecule was selected, and a ligand was chosen to dock with it.
- → The Exhaustiveness parameter of AutoDock Vina was set to 8, and the Dimensions for Vina Search Space were maximized before executing the Vina program.
- → The results for each molecule were saved in a .csv format along with snapshots of the conformations that had the least binding affinity in kcal/mol.

3. Observation of Molecular Interactions :

For visualizing the molecular interactions between ligand and target molecules, PyMOL was employed in this study. The focus was mainly on identifying the polar interactions of the molecules. The docked structures were loaded into PyMOL, and polar bonds were identified. Transparent images using Ray-Traced visualization were exported to illustrate the identified interactions.

Results

In this section results obtained in this study are represented including the images representing binding affinities [Table 1], their binding poses at minimum binding affinities and their polar interactions [Figure 8-14].

1. MEX3A

MEX3A showed binding affinity amongst highest in this study. Gossypol binds to MEX3A with binding affinity of -6.5 and it is significantly high. Thus, MEX3A is less likely to be considered as a candidate for the interaction with Gossypol. It has a single polar interaction at amino acid Arginine at the 262th position. [Figure (8)] [Table 2]

2. Ezrin

While Ezrin didn't bind with Gossypol with considerable binding affinity, these molecules bind with Gossypol with significant number of polar interactions when compared with other molecules in this study. Binding affinity for Ezrin-Gossypol complex is found -6.7 in this study. Ezrin has six sites for polar interactions with Gossypol. At the first amino acid Arginine there are three polar interactions. Glycine at 6th position is also involved in another polar interaction. Another polar interaction with Gossypol is found at 8th position that is mediated by Asparagine. At 26th position it has two polar interactions with Gossypol via Alanine. [Figure (9)] [Table 3]

3. TfR1

Lowest binding affinity of Gossypol in this study is found with TfR1. Gossypol binds to TfR1 with binding affinity of -8.3, while this affinity is more than previously studies molecules, it can be considered for the in vitro studies because interacting well with Gossypol. It has three polar interactions, with Phenyl Alanine at 212th, Tyrosin at 236th and Glutamine at 238th position in the TfR1 protein. [Figure (10)] [Table 4]

4. Cofilin1

With binding affinity of -6.9, Cofilin1-Gossypol complex is not with significant polar interaction but it can be considered to have considerable binding affinity to be the candidates that can be tested by in vitro experiments for its involvement in the regulation of ferroptosis by binding with Gossypol. Lysine at 13th position is involved in two polar interaction with Gossypol. Another Lysine at 31st position is also involved in two polar interactions with Gossypol. [Figure (11)] [Table 5]

5. ANX2

ANX2 along with COX2 is found to be having highest binding affinity with Gossypol and it's not a significant candidate for its testing to regulate ferroptosis upon binding with Gossypol. ANX2-Gossypol complex is found to be having binding affinity of -6.1 in this study. Glutamine at 36th position and Arginine at 77th position is involved in two polar interactions (one each) with the Gossypol. [Figure (12)] [Table 6]

6. HSP70

HSP70 is found to be having second lowest binding energy and potential candidate for in vitro study for its role in regulation of ferroptosis on binding with Gossypol. With the binding affinity of -7.4, HSP70-Gossypol complex is having significant polar interactions. It has three polar interactions, with Glycine at 224th, Aspartate at 225th and Tyrosin at 226th position of HSP70 protein. [Figure (13)] [Table 7]

7. COX2

In this study, it was discovered that ANX2, in combination with COX2, has the least attraction to Gossypol, and thus it is not considered a significant candidate for testing to regulate ferroptosis when binding to Gossypol. The binding affinity of the ANX2-Gossypol complex was found to be -6.1. [Figure (14)] [Table 8]

Discussion

Relatively comparable binding affinity suggest that Gossypol may show side effects as different cell types may contain these molecules in different concentrations.

The results of this study indicate that TfR1 had the lowest binding affinity, whereas ANX2 and COX2 demonstrated the highest binding affinity (Table 1). Also, all the binding affinities are significantly lower than previously studied molecules. This suggest that Gossypol might be playing crucial role in ferroptosis but it more actively participates in apoptosis as these molecules are part of central pathway of apoptosis. Also it is important to note that many of these previously studied molecules play significant role in regulation of ferroptosis such as p53[5,28,29].

One important hypothesis of this study is that Gossypol may have a significant effect on cancer cells having irregularities in the functioning of TfR1 regulation and HSP70 overexpression. This could be interrupted by Gossypol as considerable binding affinities are found for these molecules.

Conclusion

This *in-silico* study concludes the best binding affinity of Gossypol for TfR1 and HSP70. This represents the Gossypol as a potential drug candidate for the treatment of PA1 like ovarian teratocarcinoma by induction of ferroptosis. Although, other proteins are previously found to be having better binding affinities, these molecules are more closely related to regulation of ferroptosis[9]. Also, this study shows that molecules like ANX2 and COX2 are comparatively less likely to interact with gossypol and hence in the regulation of ferroptosis might not be extensively affected by these interactions. Since this study was conducted in silico, further validation is required to test the actual effects of Gossypol on various cell lines. Although the findings of this study are promising, experimental verification is necessary to move forward and confirm the results.

Figures

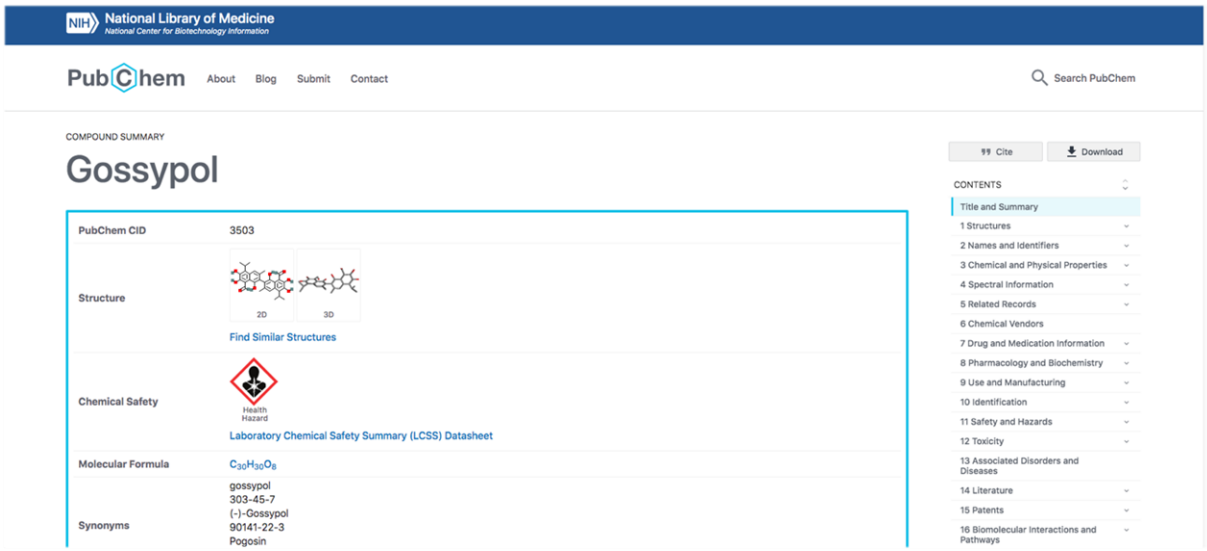

Figure (1): A screenshot of the PubChem webpage having details and download links for Gossypol

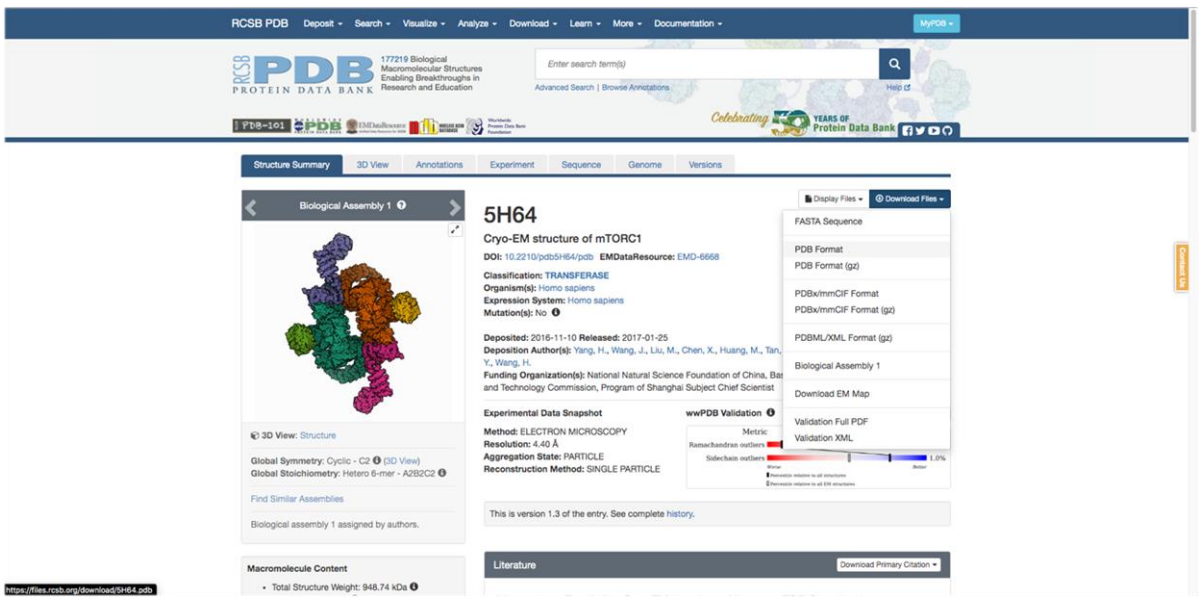

Figure (2): A screenshot of the RCSB PDB webpage having details and download links for the cryo-EM structure of mTORC1

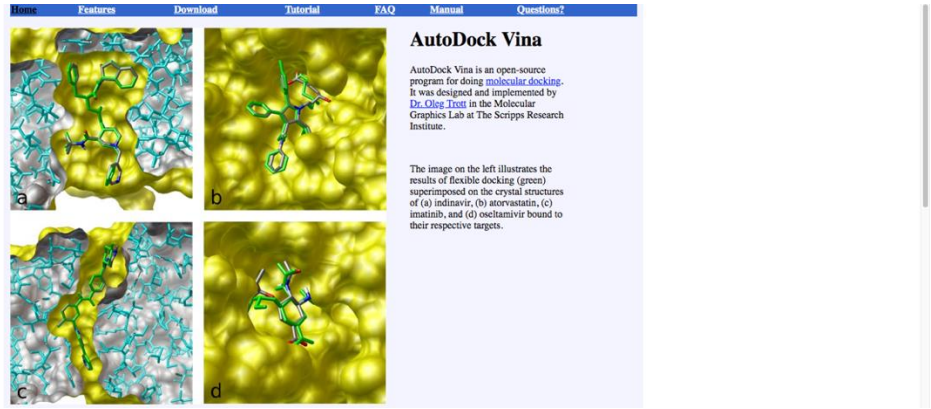

Figure (3): Screenshot of the homepage of AutoDock Vina official website

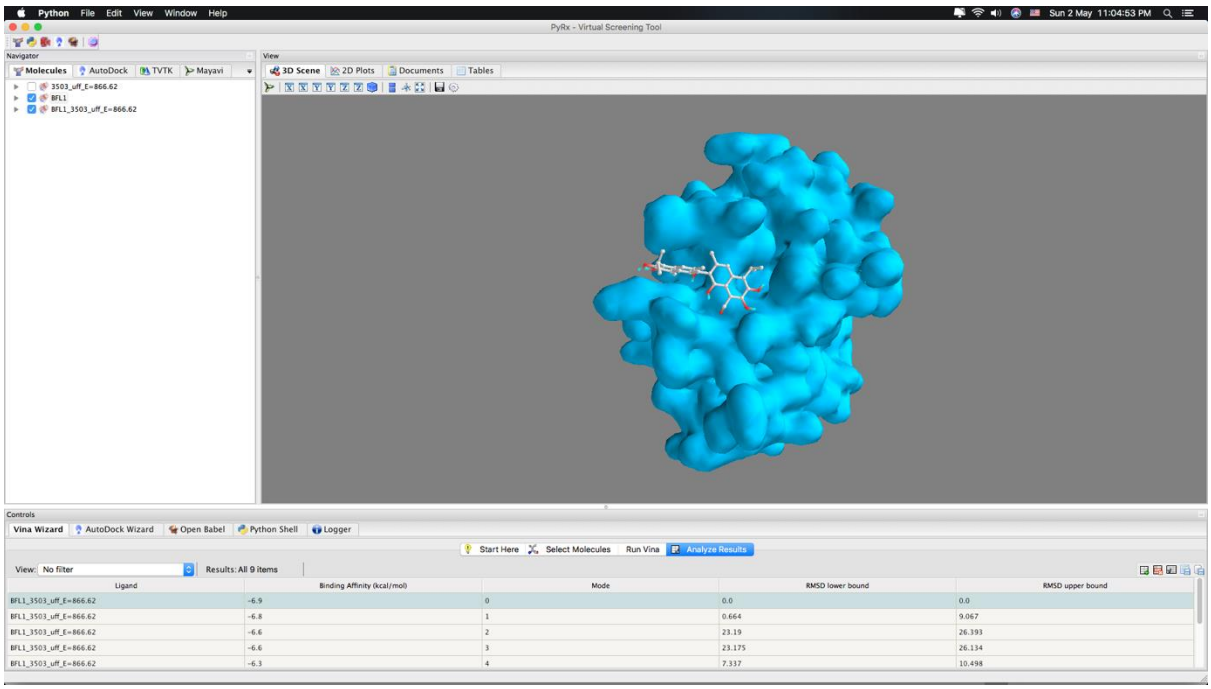

Figure (4): A screenshot showing results for three-dimensional binding of Gossypol with the BFL1 running in PyRx

Figure (5): A screenshot taken while analyzing interactions of Gossypol with the BFL1 inside PyMOL

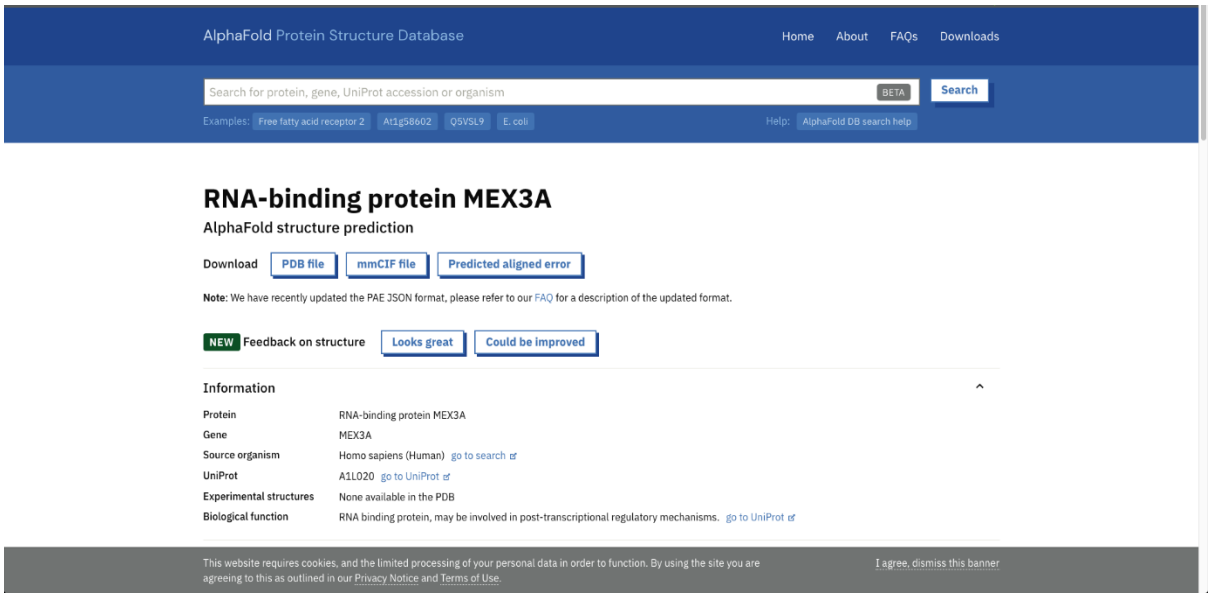

Figure (6): A screenshot taken during search of the 3D structure of MEX3A protein

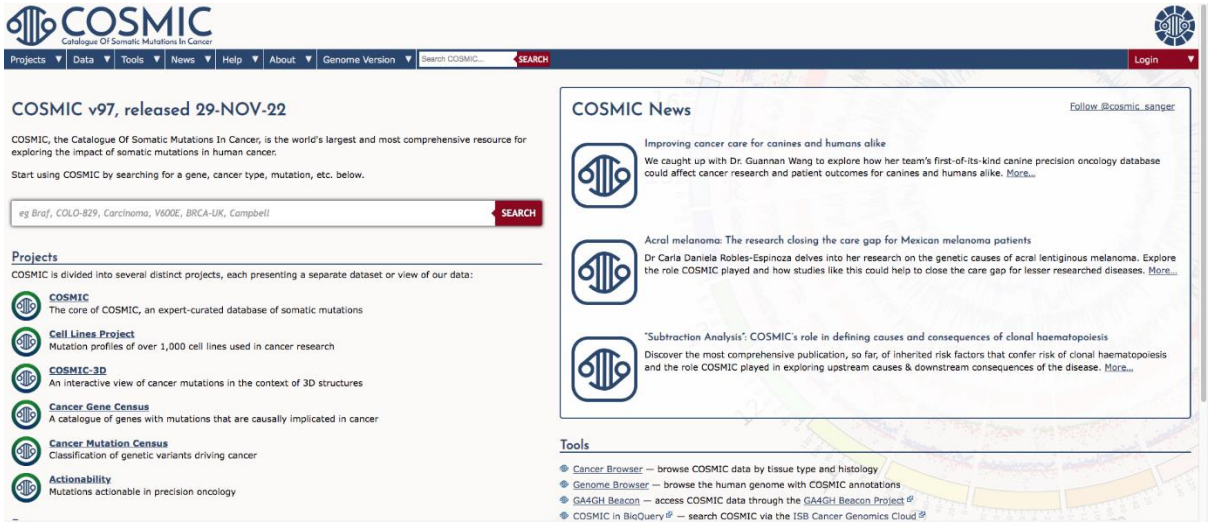

Figure (7): A screenshot of homepage of COSMIC website

Figure (8)

MEX3A & Gossypol

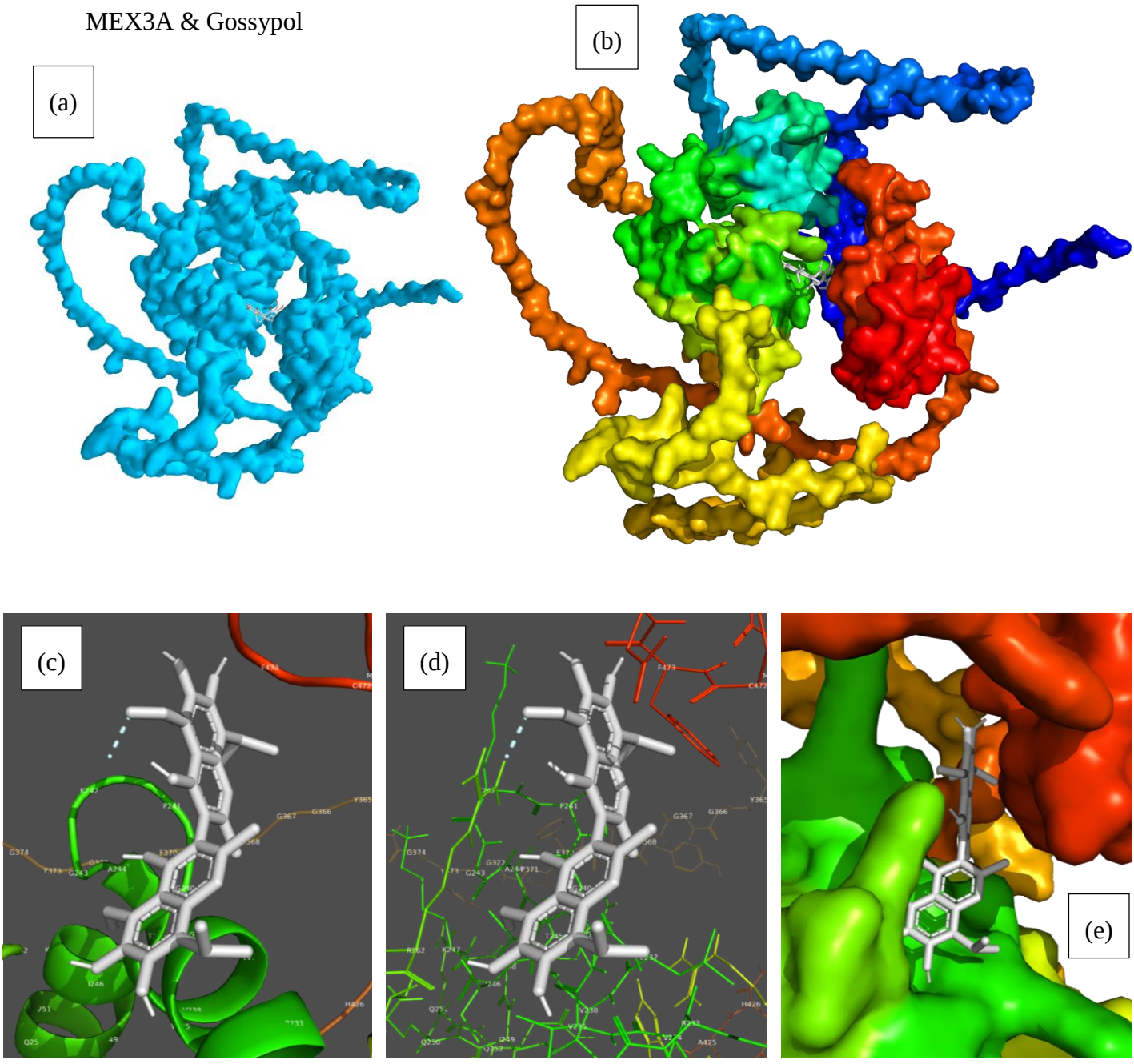

(a) Autodock vina 3D view

(b) PyMOL Vissualization

(c) Cartoon version of Gossypol interaction

(d) Wire version of Gossypol interaction

(e) Close up view of surface structure

Figure (9)

Ezrin & Gossypol

(a)

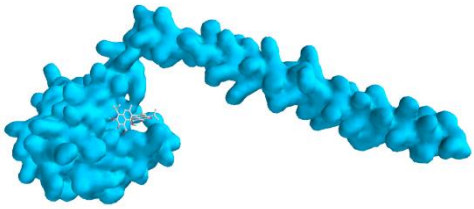

(b)

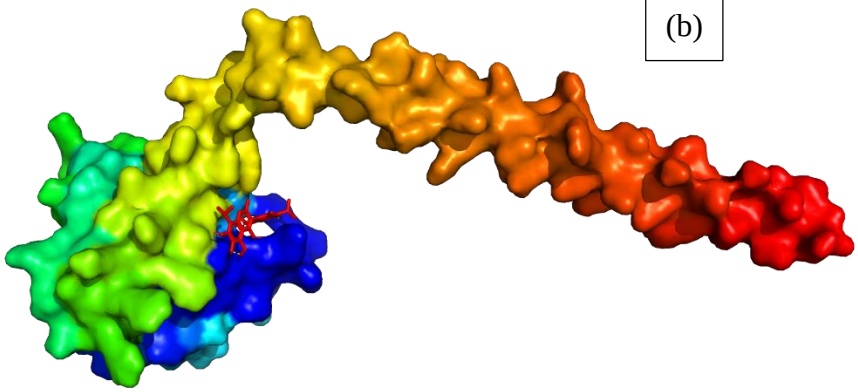

(a) Autodock vina 3D view

(b) PyMOL Vissualization

(c) Close up view of surface structure

(d) Wire version of Gossypol interaction

(e) Cartoon version of Gossypol interaction

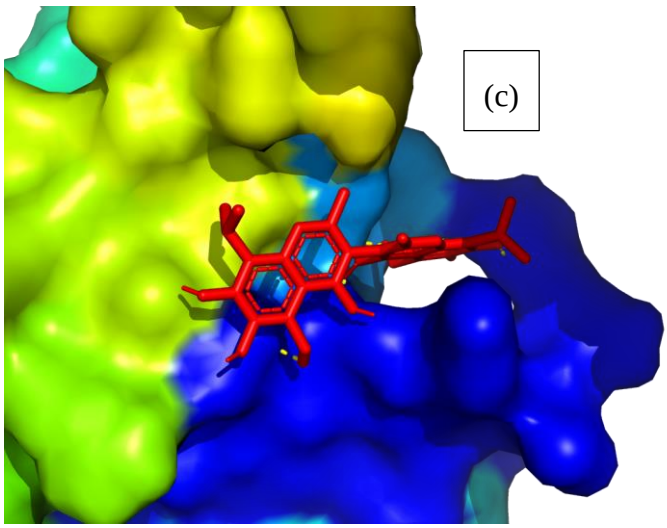

(c)

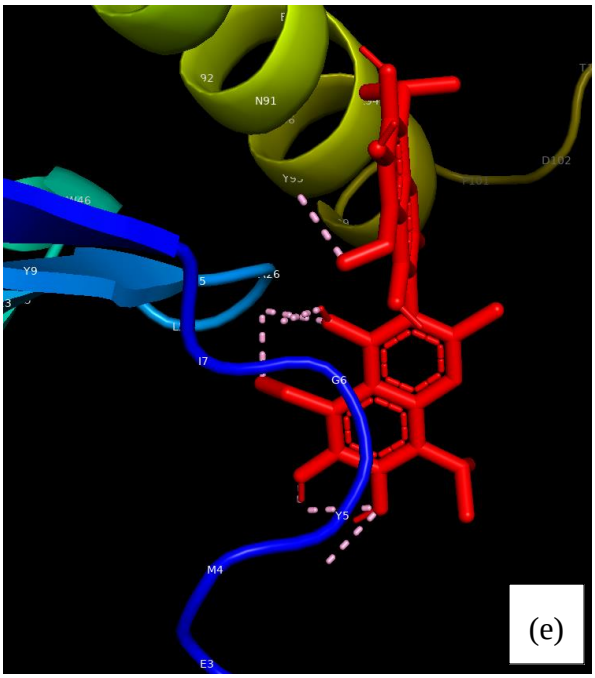

(e)

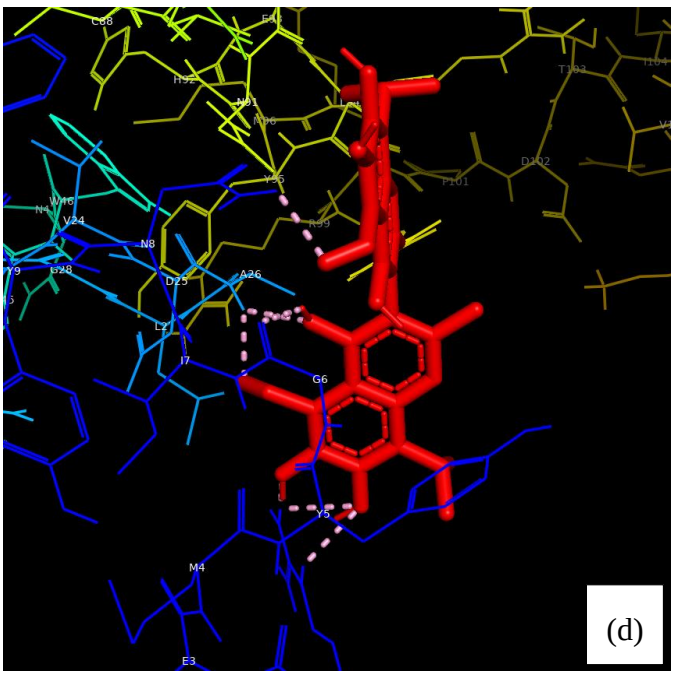

(d)

Figure (10)

TfR1 & Gossypol

(a)

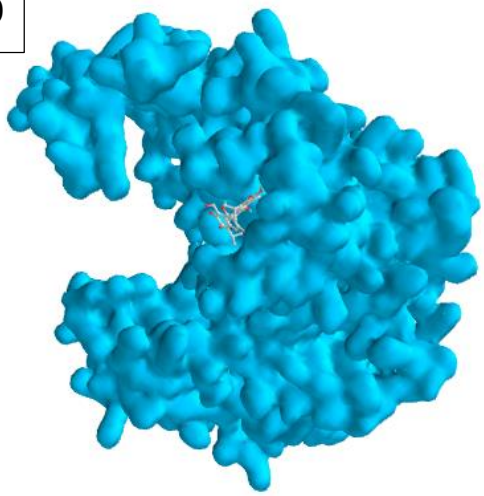

(b)

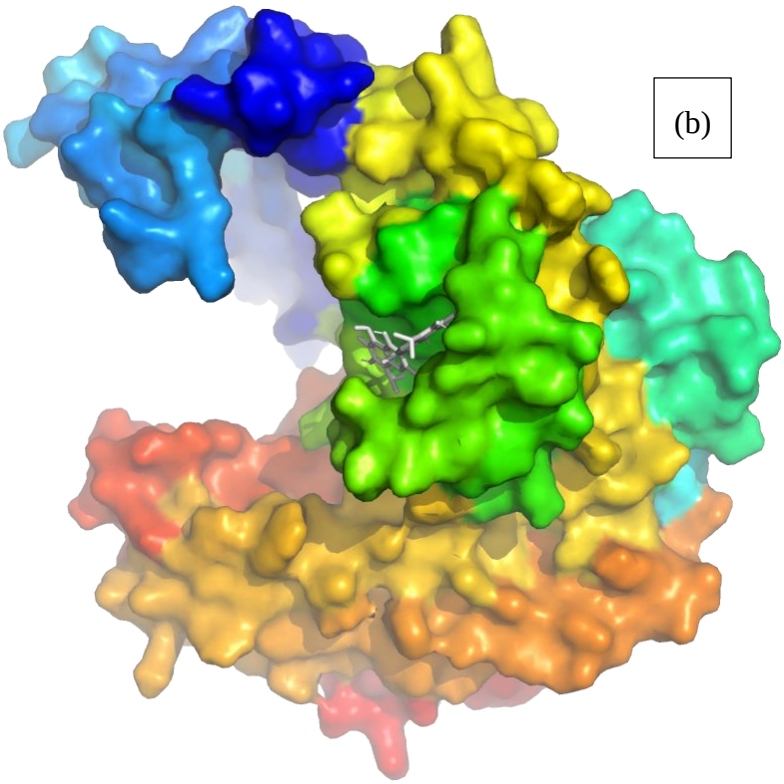

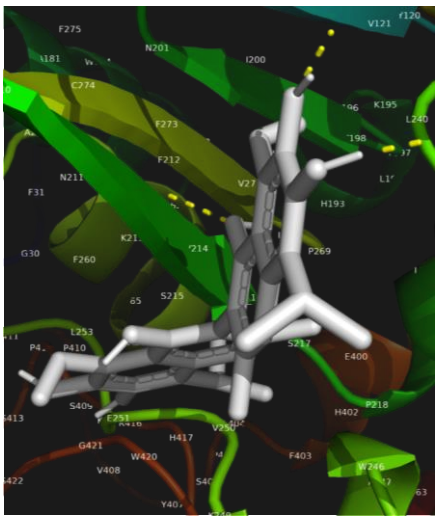

(c)

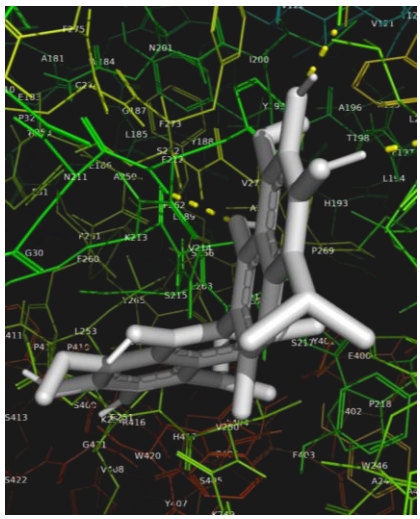

(d)

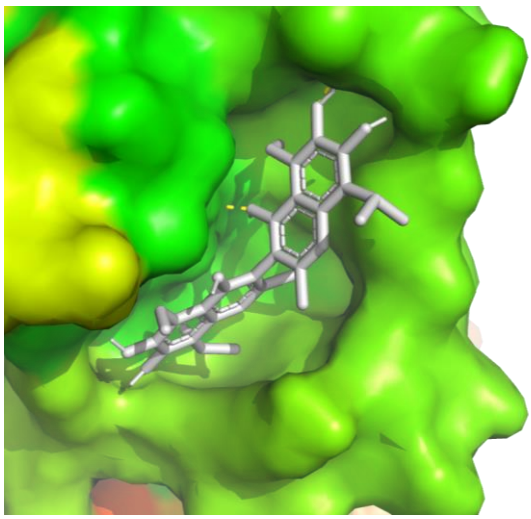

(e)

(a) Autodock vina 3D view

(b) PyMOL Vissualization

(c) Cartoon version of Gossypol interaction

(d) Wire version of Gossypol interaction

(e) Close up view of surface structure

Figure (11)

Cofilin1 & Gossypol

(a)

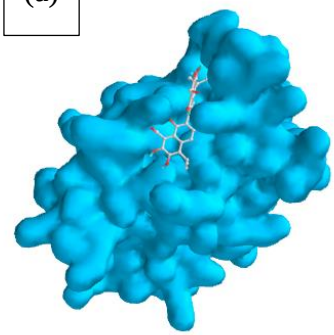

(b)

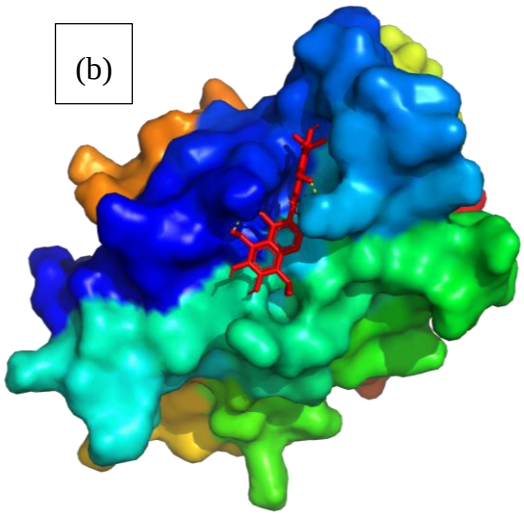

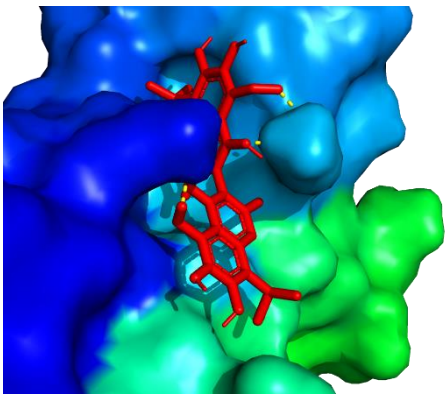

(c)

(d)

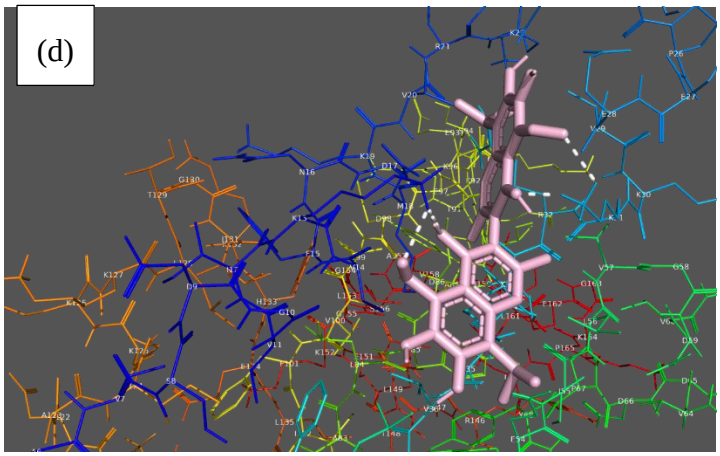

(e)

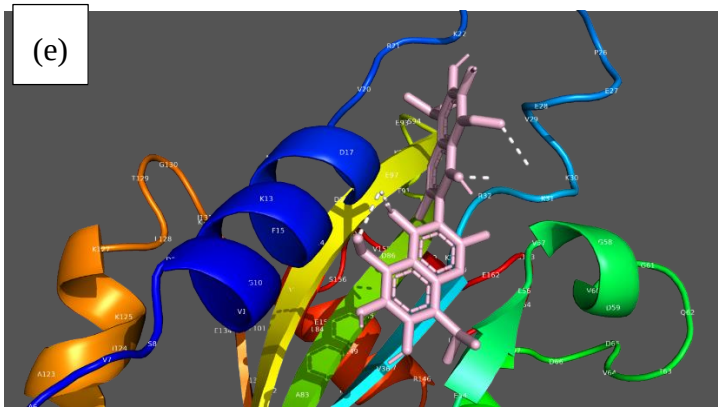

(a) Autodock vina 3D view

(b) PyMOL Vissualization

(c) Close up view of surface structure

(d) Wire version of Gossypol interaction

(e) Cartoon version of Gossypol interaction

Figure (12)

ANX2 & Gossypol

(a)

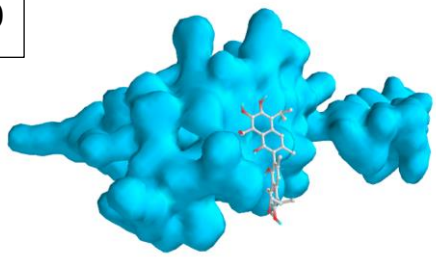

(b)

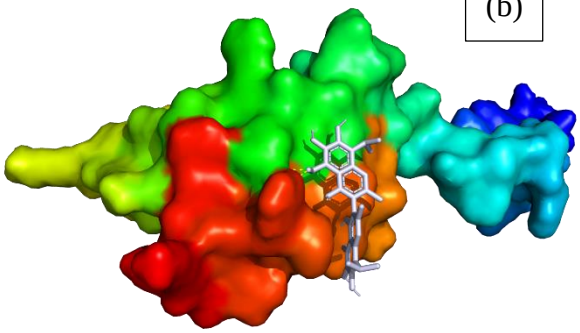

(c)

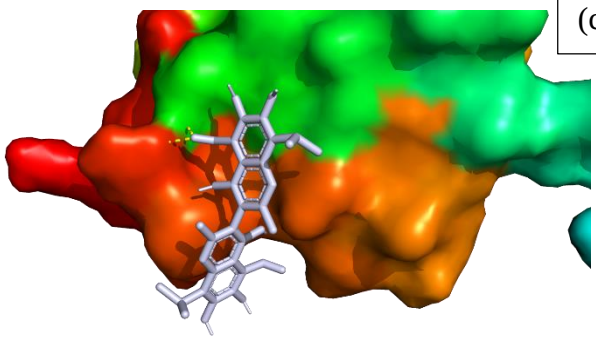

(a) Autodock vina 3D view

(b) PyMOL Vissualization

(c) Close up view of surface structure

(d) Wire version of Gossypol interaction

(e) Cartoon version of Gossypol interaction

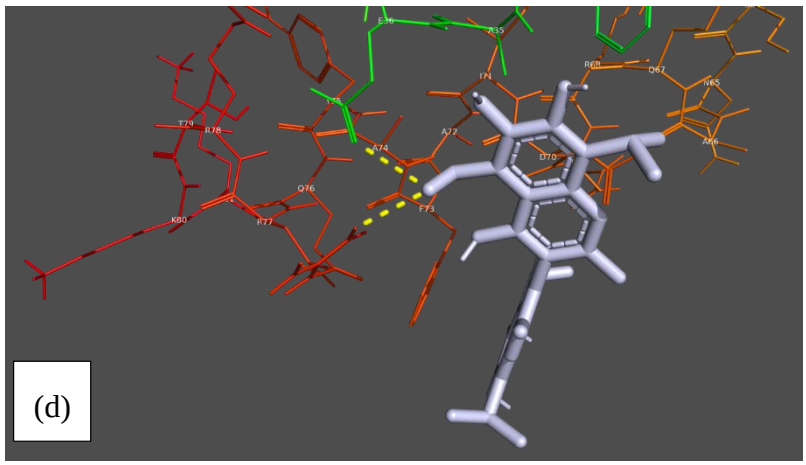

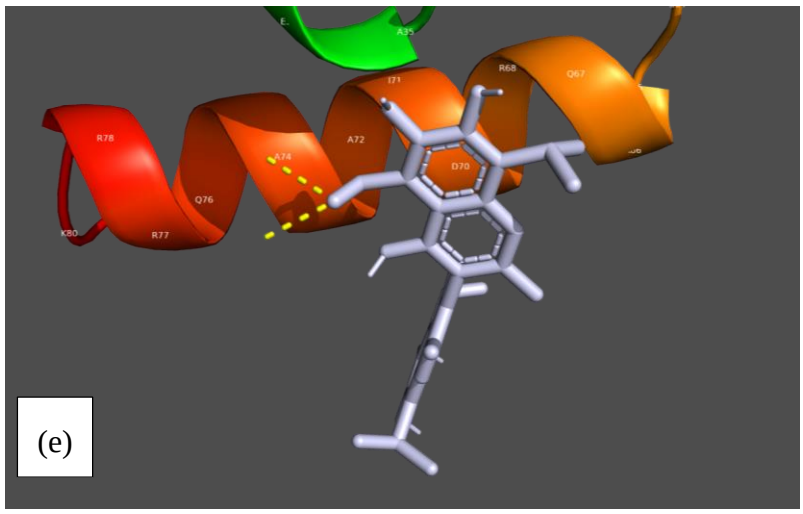

Figure (13)

HSP70 & Gossypol

(a)

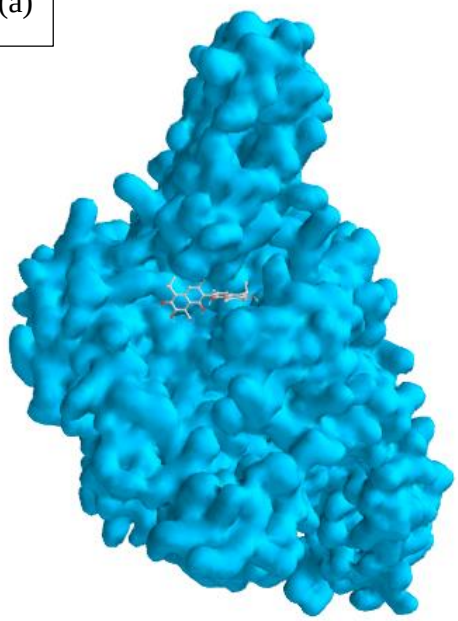

(b)

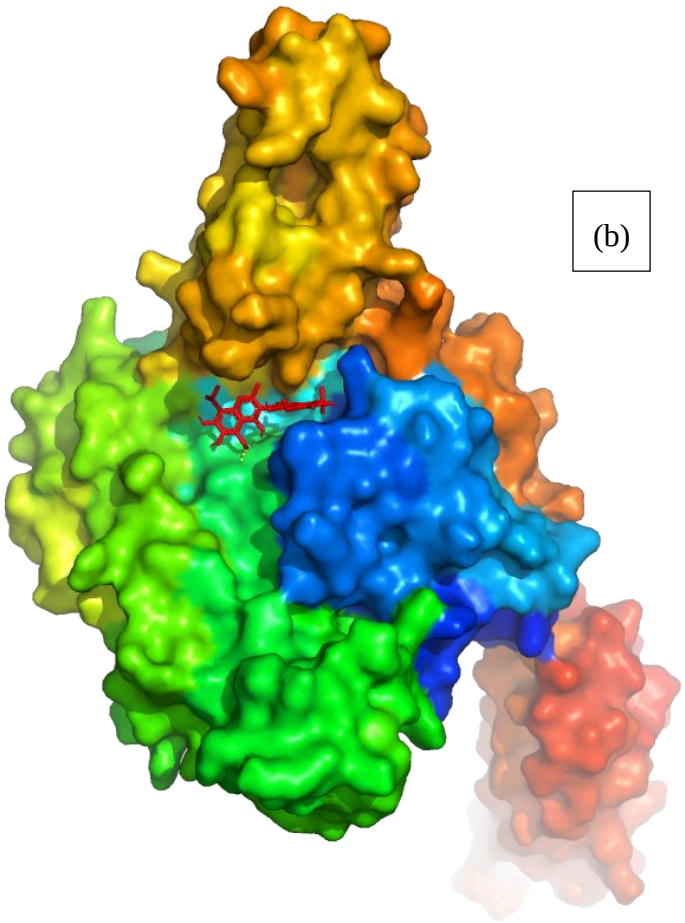

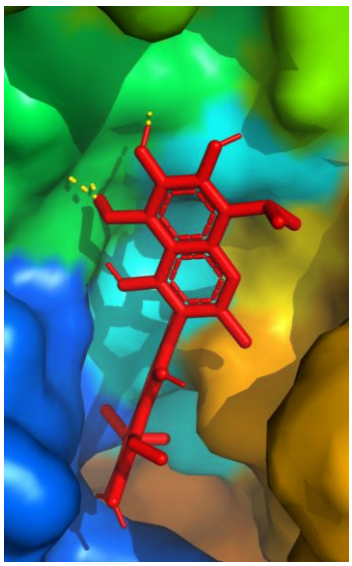

(c)

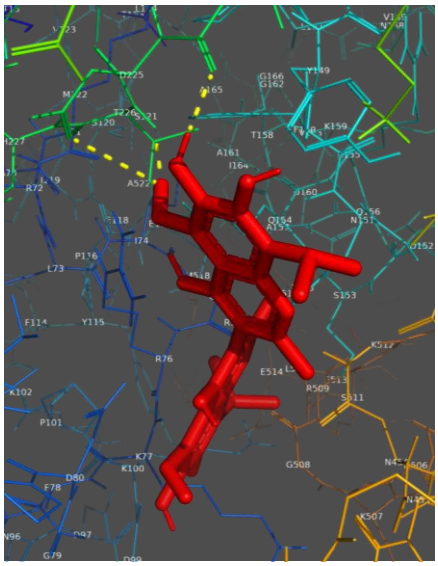

(d)

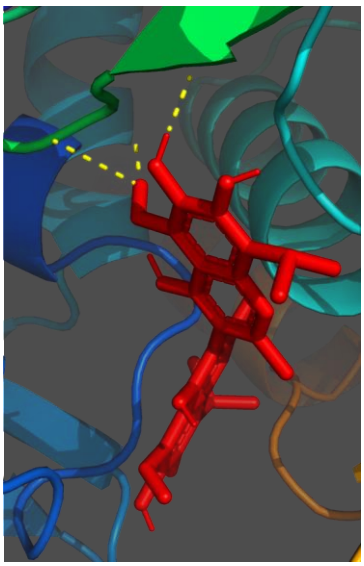

(e)

(a) Autodock vina 3D view

(b) PyMOL Vissualization

(c) Close up view of surface structure

(d) Wire version of Gossypol interaction

(e) Cartoon version of Gossypol interaction

Figure (14)

COX2 & Gossypol

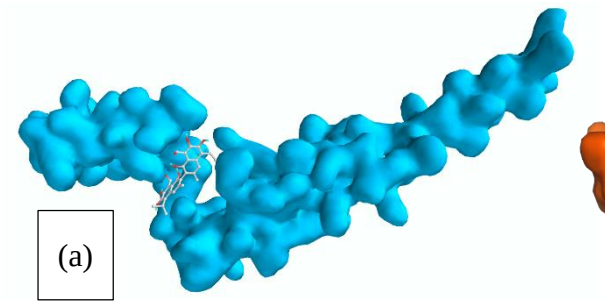

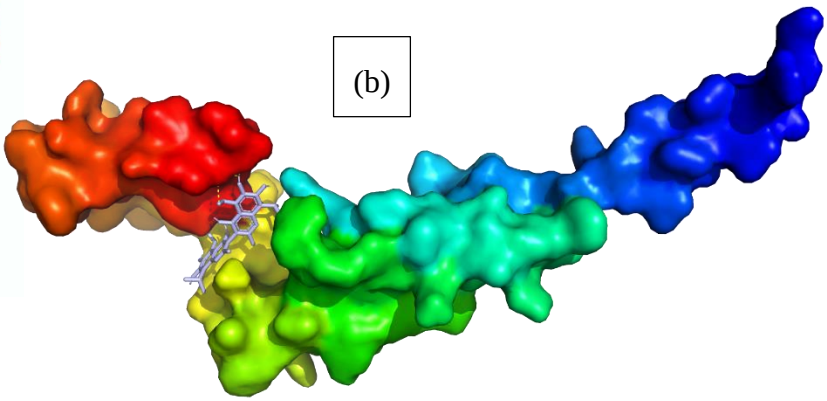

(c)

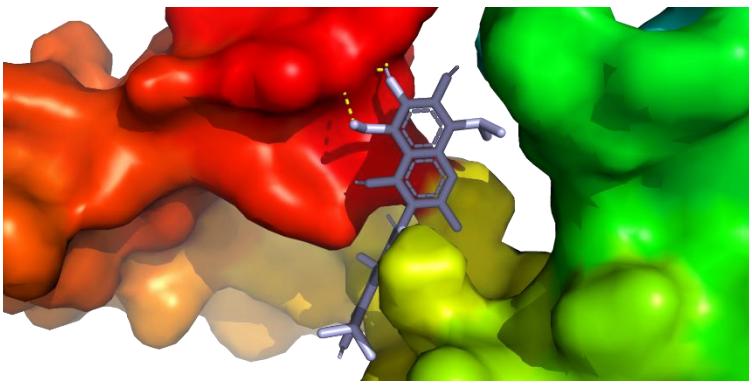

(a) Autodock vina 3D view

(b) PyMOL Vissualization

(c) Close up view of surface structure

(d) Wire version of Gossypol interaction

(e) Cartoon version of Gossypol interaction

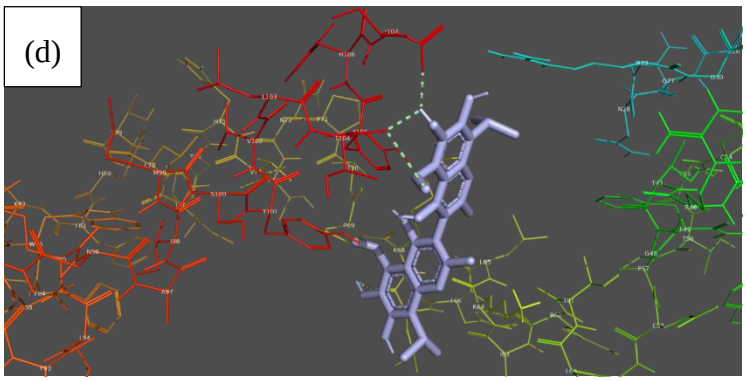

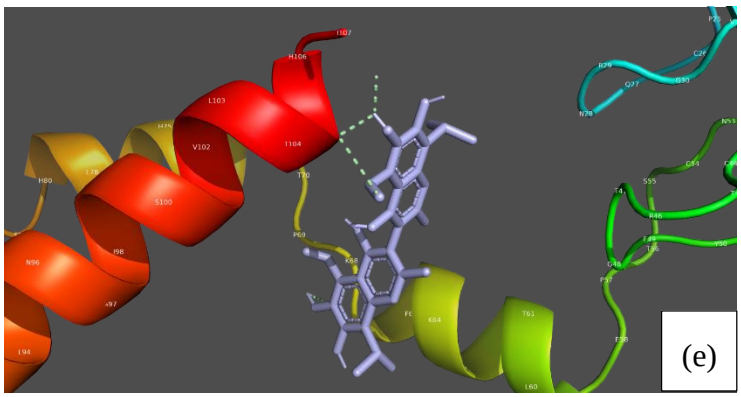

Tables

Table 1: Proteins focused in this study with their minimum binding affinity

Target	Binding Affinity
TfR1_model1_3503_uff_E=866.62	-8.3
HSP70_model1_3503_uff_E=866.62	-7.4
4bex_(Cofilin1)_3503_uff_E=866.62	-6.9
Ezrin_model1_3503_uff_E=866.62	-6.7
MEX3A_model1_3503_uff_E=866.62	-6.5
COX2_model1_3503_uff_E=866.62	-6.1
ANX2_model1_3503_uff_E=866.62	-6.1

Table 2: Binding Affinities of MEX3A with Gossypol

Ligand	Binding Affinity	rmsd/ub	rmsd/lb
MEX3A_model1_3503_uff_E=866.62	-6.5	0	0
MEX3A_model1_3503_uff_E=866.62	-6.5	8.911	0.087
MEX3A_model1_3503_uff_E=866.62	-6.3	23.792	20.647
MEX3A_model1_3503_uff_E=866.62	-6.3	12.825	9.07
MEX3A_model1_3503_uff_E=866.62	-6.3	26.378	22.367
MEX3A_model1_3503_uff_E=866.62	-6.3	12.012	8.634
MEX3A_model1_3503_uff_E=866.62	-6.3	26.922	23.671
MEX3A_model1_3503_uff_E=866.62	-6.3	8.117	4.152
MEX3A_model1_3503_uff_E=866.62	-6.2	27.723	23.077

Table 3: Binding Affinities of Ezrin with Gossypol

Ligand	Binding Affinity	rmsd/ub	rmsd/lb
Ezrin_model1_3503_uff_E=866.62	-6.7	0	0
Ezrin_model1_3503_uff_E=866.62	-6.6	9.024	0.331
Ezrin_model1_3503_uff_E=866.62	-6.5	14.743	10.321
Ezrin_model1_3503_uff_E=866.62	-6.5	14.755	10.55
Ezrin_model1_3503_uff_E=866.62	-6.3	14.509	11.855
Ezrin_model1_3503_uff_E=866.62	-6.2	14.15	11.407
Ezrin_model1_3503_uff_E=866.62	-6.2	14.434	11.504
Ezrin_model1_3503_uff_E=866.62	-6.2	7.939	4.06
Ezrin_model1_3503_uff_E=866.62	-6.2	14.294	11.819

Table 4: Binding Affinities of TfR1 mutant with Gossypol

Ligand	Binding Affinity	rmsd/ub	rmsd/lb
TfR1_model1_3503_uff_E=866.62	-8.3	0	0
TfR1_model1_3503_uff_E=866.62	-8.3	9.014	0.302
TfR1_model1_3503_uff_E=866.62	-8	4.477	2.341
TfR1_model1_3503_uff_E=866.62	-7.7	3.096	1.712
TfR1_model1_3503_uff_E=866.62	-7.6	25.506	21.594
TfR1_model1_3503_uff_E=866.62	-7.6	29.933	24.725
TfR1_model1_3503_uff_E=866.62	-7.6	26.049	21.104
TfR1_model1_3503_uff_E=866.62	-7.6	24.506	21.227
TfR1_model1_3503_uff_E=866.62	-7.5	29.09	24.729

Table 5: Binding Affinities of Cofilin1 with Gossypol

Ligand	Binding Affinity	rmsd/ub	rmsd/lb
4bex_(Cofilin1)_3503_uff_E=866.62	-6.9	0	0
4bex_(Cofilin1)_3503_uff_E=866.62	-6.9	9.169	1.782
4bex_(Cofilin1)_3503_uff_E=866.62	-6.6	17.9	14.303
4bex_(Cofilin1)_3503_uff_E=866.62	-6.5	16.561	14.275
4bex_(Cofilin1)_3503_uff_E=866.62	-6.3	21.012	17.554
4bex_(Cofilin1)_3503_uff_E=866.62	-6.3	34.659	30.059
4bex_(Cofilin1)_3503_uff_E=866.62	-6.3	20.818	17.828
4bex_(Cofilin1)_3503_uff_E=866.62	-6.1	24.05	21.111
4bex_(Cofilin1)_3503_uff_E=866.62	-6.1	20.899	15.455

Table 6: Binding Affinities ANX2 with Gossypol

Ligand	Binding Affinity	rmsd/ub	rmsd/lb
ANX2_model1_3503_uff_E=866.62	-6.1	0	0
ANX2_model1_3503_uff_E=866.62	-6	8.986	0.109
ANX2_model1_3503_uff_E=866.62	-5.9	18.597	15.247
ANX2_model1_3503_uff_E=866.62	-5.8	18.576	14.699
ANX2_model1_3503_uff_E=866.62	-5.8	18.563	15.307
ANX2_model1_3503_uff_E=866.62	-5.7	19.729	14.963
ANX2_model1_3503_uff_E=866.62	-5.6	10.356	7.293
ANX2_model1_3503_uff_E=866.62	-5.5	9.397	2.736
ANX2_model1_3503_uff_E=866.62	-5.5	22.495	17.914

Table 7: Binding Affinities of HSP70 with Gossypol

Ligand	Binding Affinity	rmsd/ub	rmsd/lb
HSP70_model1_3503_uff_E=866.62	-7.4	0	0
HSP70_model1_3503_uff_E=866.62	-7.4	3.13	1.735
HSP70_model1_3503_uff_E=866.62	-7.3	9.028	1.682
HSP70_model1_3503_uff_E=866.62	-6.8	8.848	3.09
HSP70_model1_3503_uff_E=866.62	-6.7	9.034	2.269
HSP70_model1_3503_uff_E=866.62	-6.7	5.232	3.089
HSP70_model1_3503_uff_E=866.62	-6.6	33.457	29.856
HSP70_model1_3503_uff_E=866.62	-6.6	9.552	2.635
HSP70_model1_3503_uff_E=866.62	-6.6	8.952	2.096

Table 8: Binding Affinities of COX2 with Gossypol

Ligand	Binding Affinity	rmsd/ub	rmsd/lb
COX2_model1_3503_uff_E=866.62	-6.6	0	0
COX2_model1_3503_uff_E=866.62	-6.6	9.112	0.104
COX2_model1_3503_uff_E=866.62	-6.3	19.26	17.346
COX2_model1_3503_uff_E=866.62	-6.3	20.863	17.113
COX2_model1_3503_uff_E=866.62	-6.3	13.427	10.86
COX2_model1_3503_uff_E=866.62	-6.1	3.27	1.782
COX2_model1_3503_uff_E=866.62	-6.1	5.398	2.947
COX2_model1_3503_uff_E=866.62	-6.1	8.86	3.015
COX2_model1_3503_uff_E=866.62	-6.1	8.582	3.066

Abbreviations:

ACSL4: Acyl-CoA Synthetase Long-Chain Family Member 4

ANX2: Annexin A2

APSD: AlphaFold Protein Structure Database

BRCA1/2: Breast Cancer gene 1/2

CDKN2A: Cyclin Dependent Kinase Inhibitor 2A

COX2: Cyclooxygenase 2

Cofilin1: Actin binding protein Cofilin-1

COSMIC: Catalogue Of Somatic Mutations In Cancer

GPX4: Glutathione Peroxidase 4

HSP70: Heat Shock Protein 70

KRAS: Kirsten Rat Sarcoma Viral Oncogene Homolog

MEX3A: Mex-3 RNA binding family member A

PTEN: Phosphatase and Tensin Homolog

PIK3CA: Phosphatidylinositol-4,5-Bisphosphate 3-Kinase Catalytic Subunit Alpha

RB1: Retinoblastoma 1

RCSB PDB: Research collaborator for Structural Bioinformatics Protein Data Bank

STAT: Signal Transducer and Activator of Transcription

TNBC: Triple Negative Breast Cancer

TP53: Tumor Protein 53

TfR1: Transferrin Receptor 1

mTOR: Mechanistic Target of Rapamycin

References:

1. Cancer Today. https://gco.iarc.fr/today/about.
2. Dixon, S. J. & Stockwell, B. R. The Hallmarks of Ferroptosis. *Annu. Rev. Cancer Biol.* **3**, 35–54 (2019).
3. Maru, D., Hothi, A., Bagariya, C. & Kumar, A. Targeting Ferroptosis Pathways: A Novel Strategy for Cancer Therapy. *Curr. Cancer Drug Targets* **22**, 234–244 (2022).
4. Cosmic. [No title]. https://cancer.sanger.ac.uk/cosmic/publications.
5. Wang, C. K. *et al.* MEX3A Mediates p53 Degradation to Suppress Ferroptosis and Facilitate Ovarian Cancer Tumorigenesis. *Cancer Res.* **83**, 251–263 (2023).
6. Horwitz, V. *et al.* Ezrin Is Associated with Disease Progression in Ovarian Carcinoma. *PLoS One* **11**, e0162502 (2016).
7. Zhang, S. *et al.* LncRNA KCNQ1OT1 regulates proliferation and cisplatin resistance in tongue cancer via miR-211-5p mediated Ezrin/Fak/Src signaling. *Cell Death Dis.* **9**, (2018).
8. Arumov, A. *et al.* Optimized Doxorubicin Chemotherapy for Diffuse Large B-cell Lymphoma Exploits Nanocarrier Delivery to Transferrin Receptors. *Cancer Res.* **81**, 763–775 (2021).
9. Chandrashekhar, R., Ram, B., Bhavani, L. & Bakshi, V. Molecular Docking Studies of Hydrazide-Hydrazone Derivatives of Gossypol against Bcl-2 Family Anti-Apoptotic Targets. (2017) doi:10.4172/2169-0138.1000155.
10. Tsinias, G. *et al.* High PINCH1 Expression in Human Laryngeal Carcinoma Associates with Poor Prognosis. *Anal. Cell. Pathol.* **2018**, 2989635 (2018).
11. Home - GEO - NCBI. https://www.ncbi.nlm.nih.gov/geo/.

12. Fang, C.-T., Kuo, H.-H., Hsu, S.-C. & Yih, L.-H. HSP70 is required for the proper assembly of pericentriolar material and function of mitotic centrosomes. *Cell Div.* **14**, 4 (2019).
13. Kim, C. W. *et al.* Ectopic over-expression of tristetraprolin in human cancer cells promotes biogenesis of let-7 by down-regulation of Lin28. *Nucleic Acids Res.* **40**, 3856–3869 (2012).
14. Zheng, T. *et al.* The mechanism of the Nfe2l2/Hmox1 signaling pathway in ferroptosis regulation in acute compartment syndrome. *J. Biochem. Mol. Toxicol.* **37**, e23228 (2023).
15. Klejnot, M. *et al.* Analysis of the human cofilin 1 structure reveals conformational changes required for actin binding. *Acta Crystallogr. D Biol. Crystallogr.* **69**, 1780–1788 (2013).
16. Xu, Y. *et al.* COX-2/PGE2 Pathway Inhibits the Ferroptosis Induced by Cerebral Ischemia Reperfusion. *Mol. Neurobiol.* **59**, 1619–1631 (2022).
17. Cao, H., Sethumadhavan, K. & Bland, J. M. Isolation of cottonseed extracts that affect human cancer cell growth. *Scientific Reports* **8**, 1–12 (2018).
18. Gilbert, N. E., O'Reilly, J. E., Chang, C. J. G., Lin, Y. C. & Brueggemeier, R. W. Antiproliferative activity of gossypol and gossypolone on human breast cancer cells. *Life Sciences* **57**, 61–67 (1995).
19. Messeha, S. S. *et al.* Effects of gossypol on apoptosis-related gene expression in racially distinct triple-negative breast cancer cells. *Oncology Reports* **42**, 467–478 (2019).
20. PubChem. [No title]. https://pubchem.ncbi.nlm.nih.gov/compound/Gossypol.
21. Bank, R. P. D. RCSB PDB: Homepage. https://www.rcsb.org/.
22. Trott, O. & Olson, A. J. AutoDock Vina: Improving the speed and accuracy of docking

with a new scoring function, efficient optimization, and multithreading. *J. Comput. Chem.* **31**, NA-NA (2009).

23. Dallakyan, S. & Olson, A. J. Small-molecule library screening by docking with PyRx. *Methods Mol. Biol.* **1263**, 243–250 (2015).
24. PyMOL. https://pymol.org/2/.
25. AlphaFold Protein Structure Database. https://alphafold.ebi.ac.uk/entry/A1L020.
26. Jumper, J. *et al.* Highly accurate protein structure prediction with AlphaFold. *Nature* **596**, 583–589 (2021).
27. Varadi, M. *et al.* AlphaFold Protein Structure Database: massively expanding the structural coverage of protein-sequence space with high-accuracy models. *Nucleic Acids Res.* **50**, D439–D444 (2022).
28. Feng, Z. p53 regulation of the IGF-1/AKT/mTOR pathways and the endosomal compartment. *Cold Spring Harbor perspectives in biology* vol. 2 1057–1058 Preprint at https://doi.org/10.1101/cshperspect.a001057 (2010).
29. Kang, R., Kroemer, G. & Tang, D. The tumor suppressor protein p53 and the ferroptosis network. *Free Radical Biology and Medicine* **133**, 162–168 (2019).